ISSN 1027-4510, Journal of Surface Investigation: X-ray, Synchrotron and Neutron Techniques, 2020, Vol. 14, No. 5, pp. 882–888. © Pleiades Publishing, Ltd., 2020.
Russian Text © The Author(s), 2020, published in Poverkhnost', 2020, No. 9, pp. 20–27.

Study of Silicon and the Transition Layer between Titanium and Titanium Oxide by Laser-Assisted Atom Probe Tomography

O. A. Raznitsyn[a, b, *], A. A. Lukyanchuk[a, b], I. A. Raznitsyna[a], A. S. Shutov[a, b], A. A. Khomich[a, b], V. V. Khoroshilov[a, b], A. A. Nikitin[a, b], A. A. Aleev[a, b], and S. V. Rogozhkin[a, b]

[a] *Institute for Theoretical and Experimental Physics named by A.I. Alikhanov of National Research Centre "Kurchatov Institute", Moscow, 117218 Russia*

[b] *National Research Nuclear University (MEPhI), Moscow, 115409 Russia*

**e-mail: Oleg.Raznitsyn@itep.ru*

Received December 11, 2019; revised January 14, 2020; accepted January 17, 2020

Abstract—Monitoring the characteristics of nanoscale objects is a necessary step in the development of new materials and complex low-dimensional systems. Atom-probe tomography is among the few methods that allow one to study nanoscale objects with a complex chemical composition. However, preliminary optimization of the instrument parameters is necessary for each speciment to obtain the most accurate characteristics of the materials. In this study, the results of optimization of conditions for the analysis of silicon and the titanium–titanium-oxide transition layer on a APPLE-3D atom-probe tomograph with the purpose of refining the atom-probe-tomography technique for metal–semiconductor structures are presented. The optimal laser-pulse power for studying mixtures of these materials is determined. The atomic structure of the titanium–titanium-oxide interface layer is visualized, and the concentration profiles of evaporated Ti and TiO_x ions in the transition layer are obtained.

Keywords: atom-probe tomography, mass spectrometry, microscopy, laser evaporation, silicon, titanium, titanium oxide, transition layer

DOI: 10.1134/S1027451020050158

INTRODUCTION

Modern technologies for the development of new structural materials with unique properties require the features of low-dimensional structures to be controlled, including structures at the nanoscale. Atom-probe tomography (APT) is among the methods used to study materials at this level. This method combines the principles of field ion microscopy and time-of-flight mass spectrometry applied to each atom of a speciment vaporized in strong electric fields [1]. Unlike other methods for investigating materials, APT visualizes the 3D atomic distribution structure together with determination of their chemical nature.

By virtue of its unique capabilities, APT is used to study the nanoscale features of materials with characteristic sizes of 0.3–100 nm [2]. For example, it is possible to trace, using APT, the dynamics of the growth or dissolution of nanoprecipitates and the evolution of the local chemical composition and the distribution of cluster structure elements by analyzing speciments subjected to various heat and radiation treatments [3, 4].

At present, a number of new problems of studying nanoscale features have arisen in the field of the development of devices based on complementary metal–oxide–semiconductor (CMOS) structures, which require the nanostructure, concentration, and distribution of alloying elements in the transition layers to be controlled to optimize the device characteristics, in particular, the operating speed and power consumption [5]. Indeed, the tendency toward a decrease in the scale of technological processes in manufacturing CMOS structures [6] stimulates the search for new chemical compounds with the desired electrophysical properties.

A number of problems arising when using ultrathin dielectric layers of SiO_2 (a tunneling current that exponentially increases with a decrease in the dielectric thickness, a low barrier preventing the diffusion of alloying elements, etc.) made it relevant to search for alternative materials for the gate contact of metal–oxide–semiconductor (MOS) field-effect transistors. A number of studies are known, in which titanium inclusions are used for this purpose. For example, a structure in which a TiO_2 film is separated from a silicon substrate by a thin SiO_2 layer is studied in [7]. The design, manufacturing technology, and characteristics of atomic nanophotonic silicon ring modulators coated with amorphous titanium oxide (α-TiO_2) are

presented in [8]. Ternary oxides, for example, $Ti_{0.3}Al_{0.7}O_y$ [9], were also considered as dielectrics with a high dielectric constant.

Based on the above, a material research technique capable of analyzing the existing three-dimensional structure of a material at close to atomic scale can solve problems arising in the design and further operation of promising nanostructures. Inoue et al. [10–13] studied the distribution of alloying elements in various parts of a MOS transistor and showed that APT can serve as a method for quantitative chemical and structural analysis, in particular, a method for studying the distribution of a dopant in the channel of MOS field-effect transistors, which is important for suppression of variability of the characteristics in the manufacturing of new-generation electronic devices.

The aim of this study is to refine the method for studying semiconductor structures by laser-assisted atom probe tomography, using silicon, an oxide film of titanium alloys, and titanium–titanium oxide transition layers as an example. The obtained information is intended for determining the necessary parameters of the device for studying complex structures based on silicon and titanium.

MATERIALS AND METHODS

The prototype of a laser-pulsed atom-probe tomograph (APPLE-3D) was developed at the NRC "Kurchatov Institute"—ITEP [14]. Unlike tomographs with high-voltage pulsed evaporation, this device is able to study nanoscale features not only in metals, but also in semiconductors and dielectrics [15].

When reconstructing the mass spectrum and the 3D structure of a material speciment by the APT method, a number of artifacts that reduce the accuracy of the chemical identification of atoms and which generate errors in determining the spatial coordinates of atoms can appear. The contribution of these artifacts to the reconstructed data can be reduced by varying the analysis conditions (mainly, the laser pulse power), which must be selected for each material [16, 17].

The objects of this study are silicon (purity about 99%)—which serves as the main material in the manufacture of CMOS structures—and titanium alloy Ti–6Al–4V capable of forming a durable oxide layer with a thickness of hundreds of nanometers and having low conductivity. The optimal parameters of the APT analysis for studying complex alloys were selected using the Ti–20Zr–4Al–1.5Mo alloy. The choice of these materials is determined by the task of characterizing the structural features and chemical composition of the semiconductor–conductor interface using the APT method.

The speciments were fabricated using a Helios Nanolab 600 instrument (FEI Inc., United States) with a focused ion beam (FIB) by the procedure described in [18]. The tips of the titanium-alloy speciments were not coated with any coating that could stop oxidation of the material. The silicon speciments were not subjected to additional processing.

SELECTION OF THE EVAPORATION PARAMETERS

To optimize the parameters used in the analysis of materials on a laser-pulsed atom-probe tomograph and to minimize artifacts associated with multiple events (evaporation of two or more atoms with one laser pulse), it is necessary, first of all, to select the laser power (P_{las}) for each material [17].

In some cases, it is difficult to identify the peaks of the mass spectra from different ions in complex materials because of the broadening of these peaks due to insufficient cooling of the speciment tip after a laser pulse hits (they sometimes refer to the appearance of so-called "thermal tails" on the mass spectra), which is typical for laser-assisted APT [19]. As regards the research topic addressed in this article, thermal tails from peaks of doubly ionized titanium Ti^{2+} (main peak 23.97 Da) can contribute to errors in determining the number of events of singly ionized silicon Si^+ (main peak 27.98 Da). If the evaporation conditions are selected so that singly ionized silicon Si^+ and singly ionized titanium Ti^+ (main peak 47.95 Da) are predominantly evaporated, then the mutual influence will be at the minimum level and the chemical nature of atoms of the material will be determined with maximum accuracy.

For silicon, the ratio of the number of events Si^+ to Si^{2+} was analyzed for the following P_{las} values: 1.1, 1.5, 1.9, 2.8, 4.0, and 5.9 mW. Statistical data analysis is performed for 400 thousand events per state. At the same time, the number of multiple events was monitored to make sure that it did not exceed 10% of the total number of events. The speciments were analyzed with the following instrument parameters: speciment temperature 50 K, evaporation rate 100 events/s, and laser-pulse frequency 25 kHz. The pulse duration was 300 fs. The above instrument parameters are then considered the standard parameters unless otherwise specified.

To refine the methodology for studying titanium alloys, similar laser-power selection was applied to Ti–20Zr–4Al–1.5Mo in order to analyze the dependences of the contribution of titanium ions with different degrees of ionization to the total spectrum and the number of multiple events on the laser-radiation power P_{las}. For titanium, a degree of ionization of 2^+ is

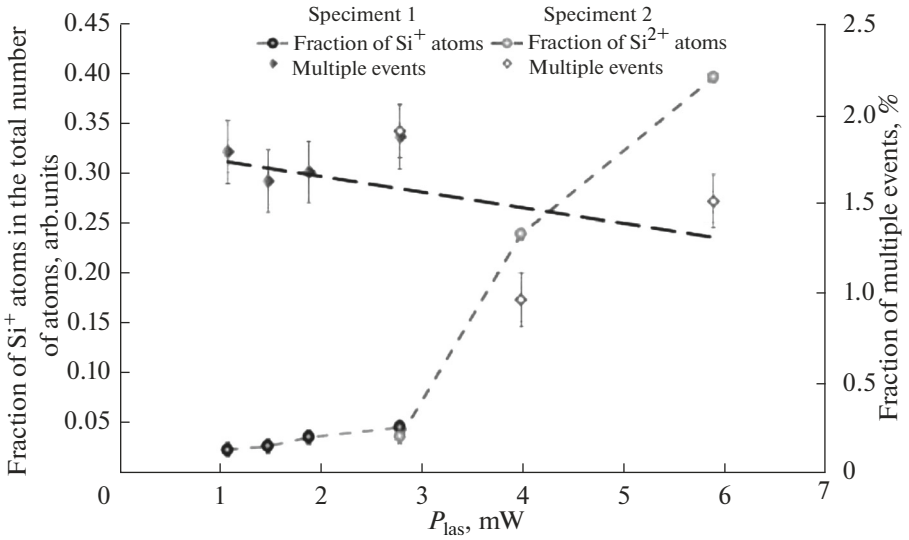

Fig. 1. Fraction of Si^+ atoms in the total number of recorded silicon atoms (main scale) and the fraction of multiple events (auxiliary scale) for two silicon speciments studied at different laser radiation powers P_{las}. The use of two speciments is determined by the need to collect sufficient statistics. The statistical variance [22] is indicated as errors. The dependence of the fraction of multiple events on the laser radiation power is approximated by a linear function for clarity.

most advantageous for evaporation [1]; therefore, the task of selecting the laser power also included exclusion of the evaporation of ions with degrees of ionization of 1^+ and 3^+. Studies were conducted with P_{las} values equal to 4, 6, 10, and 15 mW. The analyzed data statistics include 390 thousand events per state.

Ti–6Al–4V alloy, from which a speciment oxidized in air under normal conditions was prepared for the APT study, is used as the simplest model of the semiconductor–conductor structure. To visualize the features in the distribution of Ti and TiO_x, atomic maps of the transition layer were constructed. Analysis was carried out with standard parameters, with the exception of a laser power of 12.5 mW. About a million events were analyzed.

Reconstruction of the 3D atomic distribution of materials, and analysis of their mass spectra and the number of multiple events were performed using the KVANTM-3D software package developed at the NRC "Kurchatov Institute"—ITEP [20, 21].

RESULTS AND DISCUSSION

Optimization of Silicon Evaporation

Figure 1 shows the fractions of singly ionized silicon atoms in the total number of detected silicon atoms, as well as the contributions of multiple events in each study. For the selected laser-power range, the relative number of multiple events did not exceed 4% and tended to decrease with an increase in P_{las}, which indicates that the data are collected in the permissible power ranges. This trend is known in publications, including for semiconductors [23]. Due to the fact that the evaporation field for silicon is smallest for doubly ionized ions, Si^{2+} ions evaporate first [22]. Nevertheless, the obtained data show that the number of singly ionized silicon ions increases substantially with an increase in the laser radiation power to 6 mW; at the same time, the proportion of multiple events remains practically unchanged.

As can be concluded from the above, a slightly higher power might be used in studies of complex materials that contain silicon in their composition, if it is necessary for the optimal evaporation of other components of the material. For example, if the silicon matrix contains inclusions of elements for which the mass-to-charge ratio is in the range of 28–30 Da (Co^{2+}, Fe^{2+}, Mn^{2+}, etc.), then the use of low laser powers (1–2 mW) will be most beneficial under conditions that the evaporation of interesting elements also occurs with an insignificant number of multiple events (less than 10%). Otherwise, the laser power can be increased to 6 mW, which will not lead, as shown, to a failure in the chemical identification of silicon due to an increase in the number of multiple events. However, it should be noted that excessive heating of the surface of the test speciment can give rise to a decrease in the spatial resolution [24].

The mass spectrum of a silicon speciment recorded using the minimum laser radiation power is shown in Fig. 2. In this case, the mass resolution $M/\Delta M_{10\%}$ of

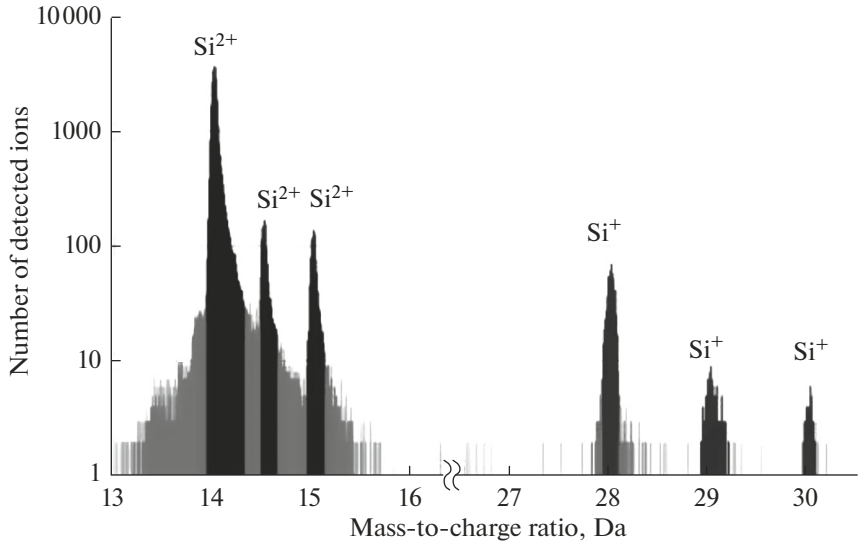

Fig. 2. Mass spectrum of the silicon speciment recorded with a laser power of 1.1 mW.

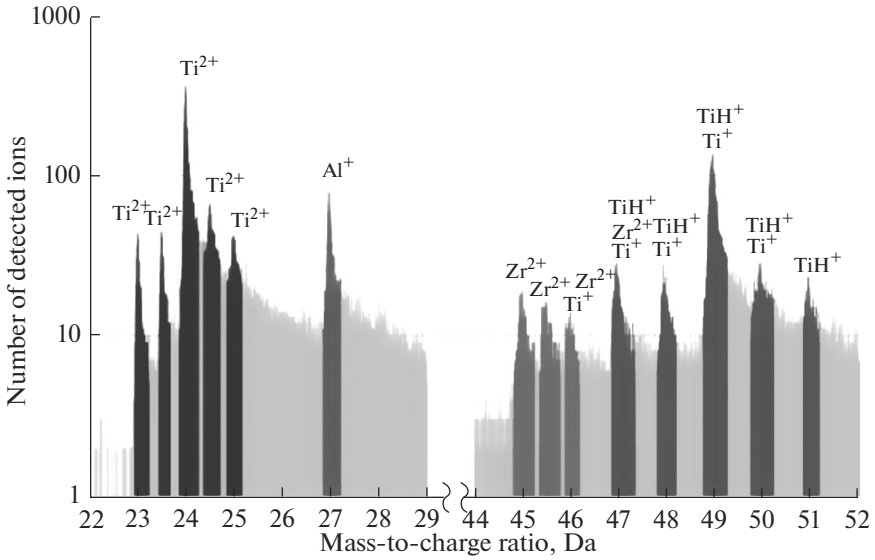

Fig. 3. Mass spectrum of the Ti–20Zr–4Al–1.5Mo alloy recorded with a laser power of 15 mW.

the main peak at a laser radiation power of 1.1 mW is 118 arb. units, and $M/\Delta M_{50\%} = 292$ a.u.

Optimization of the Parameters of Titanium-Alloy Evaporation

The characteristic mass spectrum of an investigated fragment of the Ti–20Zr–4Al–1.5Mo titanium alloy is shown in Fig. 3. As can be noted from analysis of the obtained mass spectrum, singly ionized titanium mainly evaporates in the form of a hydride. Taking into account the peculiarities of laser evaporation in APT, the following two possible reasons for this effect can be distinguished: the evaporation of hydrogen that was in the test speciment of the titanium alloy and the evaporation of residual hydrogen from the vacuum system of the APT unit. The detected hydrogen flow due to the residual content of hydrogen molecules in the chamber is a characteristic feature of laser evaporation in APT and is usually not taken into account when analyzing the composition of the tested material. In this particular case, the evaporation of titanium hydride is not a factor that violates any dependence and the evaporation of TiH^+ will be fur-

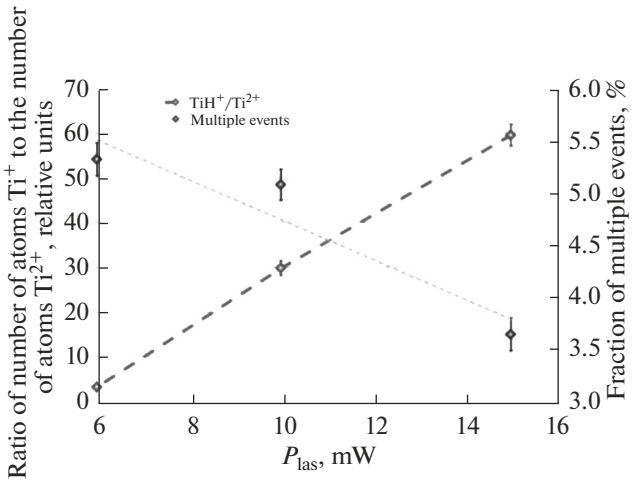

Fig. 4. Ratio of the number of Ti^+ atoms to the number of Ti^{2+} atoms (main scale) and the fraction of multiple events (auxiliary scale) for various laser powers. The statistical variance [22] and linear approximation of the dependence of the fraction of multiple events on the laser radiation power are given.

ther considered equivalent to the evaporation of Ti^+. The superposition of the mass-spectrum peaks of Zr^{2+}, Ti^+, TiH^+, and Mo^{2+}, which may complicate calculations of the real concentrations of various atoms in the speciment, is another important observation. Nevertheless, we consider the contribution of Mo atoms to this peak to be unsubstantial from the point of view of analyzing the ratio of Ti^+ and Ti^{2+} atoms, since the concentration of molybdenum in this material is about 1.5% and only 24.2% of its atoms contribute to the mass-spectrum peak at 49 Da (Fig. 3). Thus, the ratio of the number of events Ti^+ to Ti^{2+} can be calculated from their main peaks (28 and 49 Da, respectively).

It should be noted that the peaks of the main elements of the titanium alloy were difficult to identify when reducing the laser power to 4 mW, and the number of randomly evaporated atoms exceeded 85% of the total number of recorded events. Therefore, a further decrease in the laser power was not applied. The ratio of the numbers of Ti^+ and Ti^{2+} atoms and the number of multiple events for the laser-power range 6–15 mW are given in Fig. 4.

The selected range is acceptable for studying titanium alloys, since the number of multiple events under these conditions does not exceed 6%, and the main peaks of titanium are clearly distinguishable. It was found that the fraction of multiple events also decreases with an increase in the P_{las} value, as in the corresponding dependence for silicon. For conductors, this tendency was previously shown in [16].

ANALYSIS OF THE OXIDE–METAL TRANSITION LAYER OF THE Ti–6Al–4V ALLOY

To demonstrate the analysis of metal–semiconductor structures, the oxide–metal transition layer of the Ti–6Al–4V titanium alloy was studied. From this alloy, a speciment for atom-probe analysis was prepared using the FIB method. When exposed to air for about 5 h, an oxide film was formed on the speciment surface. Next, the speciment was analyzed by APT. An atom-probe image of the distribution of evaporated titanium, oxygen, and titanium-oxide ions in it is shown in Fig. 5. The concentration profiles of Ti, O, TiO, and TiO_2 ions for the selected fragment of the speciment are shown in Fig. 6.

The oxidation of titanium can yield a $TiO_{0.8}$–$TiO_{1.22}$ oxide film with a nonstoichiometric ratio of titanium and oxygen [25]. Based on the data obtained, the formed oxide evaporates mainly through the evaporation of complex TiO ions, but the evaporation of TiO_2, as well as the evaporation of titanium and oxy-

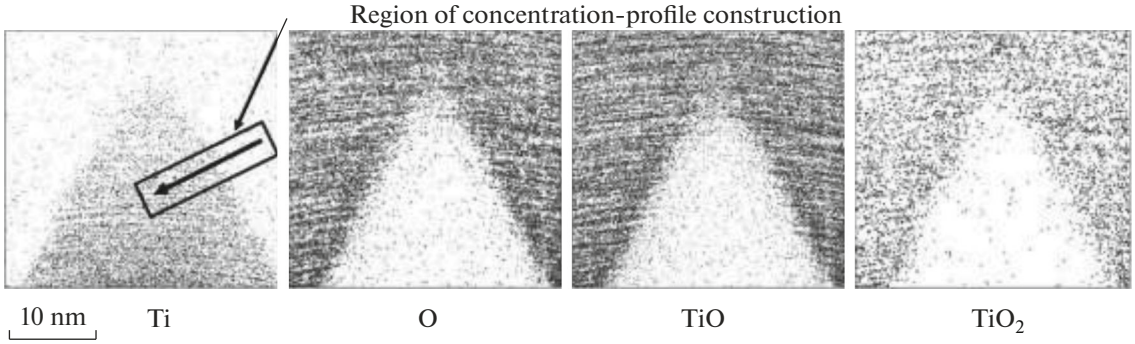

Fig. 5. Distribution of titanium and oxygen atoms in the form of evaporated Ti, O, TiO, and TiO_2 ions in the Ti–6Al–4V alloy speciment.

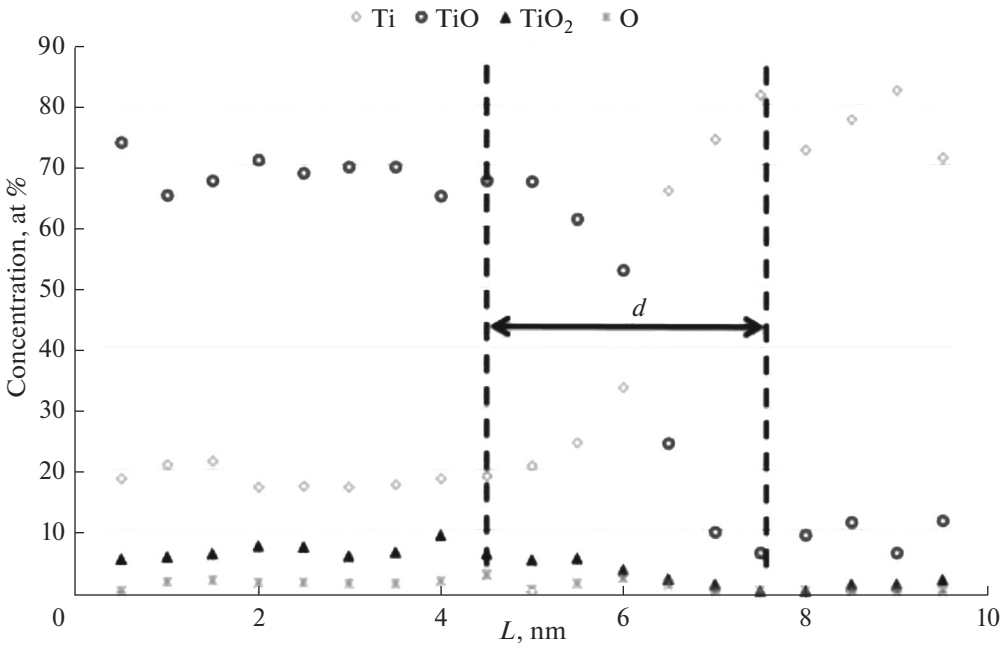

Fig. 6. Linear concentration profiles of the main chemical elements detected as Ti, O, TiO, and TiO_2 ions along the selected fragment shown in Fig. 5.

gen separately, takes place in some cases. The obtained average proportion of oxygen and titanium was about $TiO_{0.9}$. A compound with this composition is a semiconductor with a conductivity of about 10^{-4} Ω cm [25]. The thickness of the transition layer can be estimated on the basis of the obtained concentration profiles; in the selected fragment, the thickness d was approximately 3 nm (Fig. 6).

CONCLUSIONS

In this study, the data-acquisition parameters of atom-probe tomography are optimized with respect to the laser radiation power for silicon, titanium oxide, and titanium speciments by using a APPLE-3D unit. It is found that the optimal laser power for the simultaneous study of all elements of heterostructures containing silicon and titanium-alloy components is about 6 mW. The mass spectra of the studied objects are obtained, the oxide–metal transition layer of the titanium alloy is visualized, and the concentration profiles of this interfacial layer are shown. The obtained results demonstrate the applicability of devices similar to APPLE-3D for studying complex multicomponent media, including semiconductors, at nanoscale levels.

ACKNOWLEDGMENTS

The analysis of the materials by atom-probe tomography was performed using equipment of the Center for Collective Use KAMIKS (http://kamiks.itep.ru/) at the NRC "Kurchatov Institute"—ITEP.

REFERENCES

1. M. K. Miller and R. G. Forbes, *Atom-Probe Tomography: The Local Electrode Atom Probe* (Springer, London, 2014). https://doi.org/10.1007/978-1-4899-7430-3
2. P. Stender, C. Oberdorfer, M. Artmeier, P. Pelka, et al., Ultramicroscopy **107** (9), 726 (2007). https://doi.org/10.1016/j.ultramic.2007.02.032
3. S. V. Rogozhkin, N. A. Iskandarov, A. A. Lukyanchuk, A. S. Shutov, et al., Inorg. Mater.: Appl. Res. **9** (2), 231 (2018). https://doi.org/10.1134/S2075113318020247
4. S. V. Rogozhkin, A. A. Khomich, A. A. Nikitin, O. A. Raznitsyn, et al., Phys. At. Nucl. **81** (11), 1563 (2018). https://doi.org/10.1134/S1063778818120049
5. S. Kim, T. Y. Kim, K. H. Lee, T. H. Kim, et al., Nat. Commun. **8,** 15891 (2017). https://doi.org/10.1038/ncomms15891
6. W. M. Arden, Curr. Opin. Solid State Mater. Sci. **6** (5), 371 (2002). https://doi.org/10.1016/S1359-0286(02)00116-X
7. K. F. Albertin, M. A. Valle, and I. Pereyra, J. Integr. Circuits Syst. **2,** 89 (2007).
8. S. S. Djordjevic, K. Shang, B. Guan, S. T. Cheung, et al., Opt. Express **21** (12), 13958 (2013).
9. A. P. Alekhin, G. I. Lapushkin, A.M. Markeev, A. A. Sigarev, et al., J. Surf. Invest.: X-ray, Synchrotron Neutron Tech. **4,** 379 (2010).

10. K. Inoue, F. Yano, A. Nishida, T. Tsunomura, et al., Appl. Phys. Lett. **92** (10), 103506 (2008). https://doi.org/10.1063/1.2891081

11. K. Inoue, F. Yano, A. Nishida, H. Takamizawa, et al., Appl. Phys. Lett. **95** (4), 043502 (2009). https://doi.org/10.1063/1.3186788

12. K. Inoue, F. Yano, A. Nishida, H. Takamizawa, et al., Ultramicroscopy **109** (12), 1479 (2009). https://doi.org/10.1016/j.ultramic.2009.08.002

13. H. Takamizawa, Y. Shimizu, K. Inoue, T. Toyama, et al., Appl. Phys. Lett. **99** (13), 133502 (2011). https://doi.org/10.1063/1.3644960

14. S. V. Rogozhkin, A. A. Aleev, A. A. Lukyanchuk, A. S. Shutov, et al., Instrum. Exper. Tech. **60** (3), 428 (2017). https://doi.org/10.1134/S002044121702021X

15. T. F. Kelly and M. K. Miller, Rev. Sci. Instrum. **78** (3), 031101 (2007). https://doi.org/10.1063/1.2709758

16. O. A. Raznitsyn, A. A. Lukyanchuk, A. S. Shutov, S. V. Rogozhkin, et al., J. Anal. Chem, **72** (14), 1404 (2017). https://doi.org/10.1134/S1061934817140118

17. O. A. Raznitsyn, A. A. Lukyanchuk, A. S. Shutov, S. V. Rogozhkin, et al., Yad. Fiz. Inzhin. **8** (2), 138 (2017). https://doi.org/10.1134/S2079562917020208

18. V. V. Khoroshilov, O. A. Korchuganova, A. A. Lukyanchuk, O. A. Raznitsyn, et al., J. Surf. Invest.: X-ray, Synchrotron Neutron Tech. **12** (1), 87 (2018). https://doi.org/10.1134/S1027451017060106

19. T. F. Kelly, A. Vella, J. H. Bunton, J. Houard, et al., Curr. Opin. Solid State Mater. Sci. **18** (2), 81 (2014). https://doi.org/10.1016/j.cossms.2013.11.001

20. A. S. Shutov, A. A. Lukyanchuk, S. V. Rogozhkin, O. A. Raznitsyn, et al., Yad. Fiz. Inzhin. **8** (2), 141 (2017). https://doi.org/10.1134/S2079562917020221

21. A. A. Aleev, S. V. Rogozhkin, A. A. Lukyanchuk, A. S. Shutov, et al., State Certificate No. 2018661876 of Computer Software Registration (20 September 2018) [in Russian].

22. B. Gault, M. P. Moody, J. M. Cairney, and S. P. Ringer, *Atom Probe Microscopy,* Vol. 160 of *Springer Series in Material Science* (Springer, New York, 2012). https://doi.org/10.1007/978-1-4614-3436-8

23. M. Muller, D. W. Saxey, G. D. W. Smith, and B. Gault, Ultramicroscopy **111,** 487 (2011).

24. A. Cerezo and P. H. Clifton, Ultramicroscopy **107,** 720 (2007).

25. V. B. Lazarev, V. V. Sobolev, and I. S. Shaplygin, *Chemical and Physical Properties of Simple Metal Oxides* (Nauka, Moscow, 1983) [in Russian].

Translated by O. Kadkin